Abnormal Brain Topological Structure of Mild Depression During Visual Search Processing Based on EEG Signals

Shuting Sun, Liangliang Liu, Xuexiao Shao, Chang Yan, Xiaowei Li, *Member, IEEE*, and Bin Hu, *Senior Member, IEEE*

***Abstract*— Studies have shown that attention bias can affect behavioral indicators in patients with depression, but it is still unclear how this bias affects the brain network topology of patients with mild depression (MD). Therefore, a novel functional brain network analysis and hierarchical clustering methods were used to explore the abnormal brain topology of MD patients based on EEG signals during the visual search paradigm. The behavior results showed that the reaction time of MD group was significantly higher than that of normal group. The results of functional brain network indicated significant differences in functional connections between the two groups, the amount of inter-hemispheric long-distance connections are much larger than intra-hemispheric short-distance connections. Patients with MD showed significantly lower local efficiency and clustering coefficient, destroyed community structure of frontal lobe and parietal-occipital lobe, frontal asymmetry, especially in beta band. In addition, the average value of long-distance connections between left frontal and right parietal-occipital lobes presented significant correlation with depressive symptoms. Our results suggested that MD patients achieved long-distance connections between the frontal and parietal-occipital regions by sacrificing the connections within the regions, which might provide new insights into the abnormal cognitive processing mechanism of depression.**

***Index Terms*— Mild depression, EEG, functional brain network, tree agglomerative hierarchical clustering, visual search.**

Manuscript received 14 January 2022; revised 14 April 2022 and 17 May 2022; accepted 6 June 2022. Date of publication 27 June 2022; date of current version 1 July 2022. This work was supported in part by the National Key Research and Development Program of China under Grant 2019YFA0706200; in part by the National Natural Science Foundation of China under Grant 61632014, Grant 61627808, and Grant 61210010; in part by the National Basic Research Program of China (973 Program) under Grant 2014CB744600; in part by the Program of Beijing Municipal Science and Technology Commission under Grant Z171100000117005; in part by the Typical Application Demonstration Project of Shandong Academy of Intelligent Computing Technology under Grant SDAICT2081020; and in part by the Fundamental Research Funds for the Central Universities under Grant lzujbky-2017-it74, Grant lzujbky-2017-it75, Grant lzujbky-2019-26, and Grant lzuxxxy-2019-t. *(Shuting Sun and Liangliang Liu contributed equally to this work.) (Corresponding authors: Bin Hu; Xiaowei Li.)*

This work involved human subjects or animals in its research. Approval of all ethical and experimental procedures and protocols was granted by the Ethics Committee of the School of Psychology of Beijing Normal University, and performed in line with the Declaration of Helsinki.

Shuting Sun is with the Gansu Provincial Key Laboratory of Wearable Computing, School of Information Science and Engineering, Lanzhou University, Lanzhou 730000, China, and also with the Brain Health Engineering Laboratory, Institute of Engineering Medicine, Beijing Institute of Technology, Beijing 100811, China (e-mail: sunsht17@lzu.edu.cn).

Liangliang Liu and Xuexiao Shao are with the Gansu Provincial Key Laboratory of Wearable Computing, School of Information Science and Engineering, Lanzhou University, Lanzhou 730000, China (e-mail: liull2020@lzu.edu.cn; shaoxx19@lzu.edu.cn).

Chang Yan is with the Brain Health Engineering Laboratory, Institute of Engineering Medicine, Beijing Institute of Technology, Beijing 100811, China (e-mail: ychang0212@bit.edu.cn).

Xiaowei Li is with the Gansu Provincial Key Laboratory of Wearable Computing, School of Information Science and Engineering, Lanzhou University, Lanzhou 730000, China, and also with the Shandong Academy of Intelligent Computing Technology, Jinan 250000, China (e-mail: lixwei@lzu.edu.cn).

Bin Hu is with the Gansu Provincial Key Laboratory of Wearable Computing, School of Information Science and Engineering, Lanzhou University, Lanzhou 730000, China, also with the Brain Health Engineering Laboratory, Institute of Engineering Medicine, Beijing Institute of Technology, Beijing 100811, China, also with the CAS Center for Excellence in Brain Science and the Institutes for Biological Sciences, Shanghai Institutes for Biological Sciences, and the Joint Research Center for Cognitive Neurosensor Technology of Lanzhou University and Institute of Semiconductors, Chinese Academy of Sciences, Beijing 100045, China, and also with the Engineering Research Center of Open Source Software and Real-Time System (Lanzhou University), Ministry of Education, Lanzhou 730000, China (e-mail: bh@lzu.edu.cn).

This article has supplementary downloadable material available at https://doi.org/10.1109/TNSRE.2022.3181690, provided by the authors.

Digital Object Identifier 10.1109/TNSRE.2022.3181690

I. Introduction

DEPRESSION is a mental illness common to all human beings in society. According to World Health Organization (WHO), there are approximately 300 million people suffering from depression worldwide, and it may become the world's number one disease in 2030 [1]. Depression includes a variety of symptoms and signs, physical aspects mainly include sleep disturbance, appetite changes, fatigue, slow psychomotor and agitation, while psychological aspects mostly contain loss of self-esteem, feelings of guilt, inability to concentrate, and thoughts of suicide and self-harm, etc [2]. According to domestic survey, the suicide rate of depression is about 20 times higher than that of the general population [3]. In recent years, the incidence of depression (and suicide) began to show a trend of younger age (college students, even primary and secondary school students) [4]. Mild depression (MD) is more common than major depressive disorder in daily life and may increase in severity over time [5]. However, it receives much less attention than major depressive disorder. At present, there is no objective and quantitative method for detection and treatment of mild depression that can help MD patients to

take precautions and avoid developing into major depression. The most widely used diagnostic criteria for depression are based on the Diagnostic and Statistical Manual of Mental Disorders-IV (DSM-IV) [6] and International Classification of Diseases-10 (ICD-10) [7]. Influenced by doctors' proficiency and patients' cooperation, traditional diagnostic methods show strong subjectivity and low sensitivity [8]. Therefore, early identification and exploration of abnormal neural mechanisms especially of mild depression, are key issues to be solved.

Electroencephalogram (EEG) is a method of recording brain activity using electrophysiological indicators, resulting from the summations of postsynaptic potentials generated by a large number of neuronal synchronization during brain activity. EEG records the electrical wave changes during brain activity and is the overall reflection of electrophysiological activities of brain nerve cells on the cerebral cortex or scalp [9]. Due to its high time resolution ($<$1ms) [10], non-invasiveness, relatively low cost, portability and etc., EEG technology has been widely used to assess the brain functional connection mode of depressive patients in the resting state [11], [12].

Traditional functional connection analysis was based on the weighted functional connection matrix. Although some findings have been obtained, for example, compared to normal controls, depressive patients had higher functional connectivity in different frequency bands [13], [14], more and more studies are based on binary functional brain networks. Because binarization methods can not only alleviate the noise level, but also reveal the main topological structure of potential brain activity [15]. At present, the unbiased binarization technique minimum spanning tree (MST) method is often used in research, since it can overcome the problem of subjective deviation and inconsistent number of edges caused by threshold selection [16], [17]. But there still remain some disadvantages, for example, it will lead to a high degree of sparse network, which may leave out the information about the network topology. In addition, it may also include weaker brain functional network connections, which may obscure the potential network topology. Therefore, we choose a novel and unbiased cluster span threshold (CST) method. It sets the threshold by balancing the ratio of closed and open triples, rather than fixing the connection density at an arbitrary value [18]. CST captures differences found at high and low threshold levels, which may make different network metrics more sensitive [19]. This method has been proved effective in our previous studies on depression [15], but whether this method can capture the subtle changes of network topology in patients with mild depression will be a problem to be explored in this study.

Clustering and hierarchical clustering organization reveal the main building blocks of the brain network correspond to specialized brain functions [20]. In the brain network, the cluster or community structure is defined as a subset of highly interconnected nodes with similar characteristics [21]. Previous studies have shown that brain networks are hierarchical and modular [8], [15]. Constructing the hierarchical modularity of the brain, hierarchical clustering is a special method that represents the main components or hierarchical modularity of the brain network [22]. Some recent studies have found that the use of a tree agglomerated hierarchical clustering (TAHC) method can effectively detect clusters in the MST of artificial trees and weighted social networks [23], [24]. However, as the previously mentioned CST method has certain advantages over MST, we propose to apply TAHC method to the functional brain network constructed based on CST, hoping to capture a more significant modular structure of the network topology of the mild depressive patients.

The visual search paradigm generally requires subjects to search for and respond to a specified target in several distractors. This is a top-down, conscious cognitive processing task [25]. The visual search paradigm can distinguish between attentional alertness and attentional disengagement difficulties. At present, the experiments on attention-biased visual search are usually divided into two categories. One is to search for neutral targets in emotional distractions, which mainly examines the ability to disarm attention. If searching for a neutral stimulus in the emotional matrix is slower than searching for another neutral stimulus in the neutral matrix, that means it is difficult to pay attention to the emotional stimulus. Hahn *et al.* investigated the role of emotional faces as distractors by comparing the search for neutral faces between happy faces and angry faces, they found both younger and older adults showed a more effective search when the discrepant face was angry rather than happy or neutral [26]. The other type is searching for emotional targets in neutral distractors, mainly to investigate attention and alertness. If searching for an emotional stimulus in the neutral matrix is faster than searching for another neutral stimulus in the neutral matrix, it indicates that there is alertness to the emotional stimulus. Traits of anxious people's visual search experiments found that searching for sad faces in neutral faces was faster than happy faces, indicating that people with trait of a higher level of anxieties have negative attentional alertness [27]. Previous researches mainly studied the abnormal attention bias of depression patients based on behavioral indicators [28]-[29]. However, it is still unclear whether this bias affects the whole brain networks topology of MD patients. Therefore, this study chose to analyze the abnormal attention bias of MD patients based on functional brain network metrics in the visual search task.

In this study, the EEG signals of 24 MD patients and 24 normal controls (NC) subjects were recorded under the visual search paradigm. The main work includes the following aspects: Firstly, behavioral data analysis is carried out, including reaction time and accuracy. Secondly, the differences in functional connection matrix and network properties (e.g. Edge Betweenness Centrality, Node Betweenness Centrality) between MD patients and NC subjects are studied. Then, we use TAHC algorithm to observe the abnormal modular structure of MD patients, and analyze the brain asymmetry problem. Finally, we assessed the potential relationships between network metrics and clinical symptoms.

In summary, the main contributions of this study are three folds: 1) This study adopted novel functional brain network analysis method and hierarchical clustering algorithm for the first time to systematically explore the abnormal brain topology of patients with MD based on EEG signals, which could ensure a trade-off of sparsity and density of network structure,

TABLE I
STATISTICAL RESULTS OF DEMOGRAPHIC VARIABLES OF MD PATIENTS AND NC SUBJECTS

Characteristic	MD (n = 24)		NC (n = 24)		p-value
	Mean	Std	Mean	Std	
Age	22.54	2.17	23.79	2.00	0.523
Gender (Female/Male)	18/6		15/9		0.525
Education	3.25	1.70	4.00	1.53	0.410
BDI	16.17	5.92	3.67	2.70	**<0.001**

[1] Independent sample t test was used for age, education, and BDI. Chi-square test was used for gender. The statistical value was $p<0.05$. Std is the standard deviation.

and then capture the subtle differences of topology changes. 2) This is the first study combined behavioral indicators and brain network metrics to comprehensively characterize attentional bias in patients with MD during the visual search paradigm. 3) This study explored potential relationships between network metrics and clinical symptoms. It was found that the average value of long-distance connections between left frontal and right parietal-occipital lobes presented significant correlation with depressive symptoms, which might provide the underlying biomarkers for probable MD identification.

II. MATERIALS AND METHODS

In this section, we will introduce the data and methods used in this study. The major abbreviations notations used in this paper were shown in the supplementary materials V.

A. Participants

In this study, 48 subjects from Lanzhou University were participated in the experiment. All subjects completed the psychological screening system and received an interview with a psychologist. According to the psychologist, 24 subjects were considered depressed and 24 subjects were considered normal. All of them had no prior history of mental disorder and normal or corrected-to-normal vision. In addition, participants were asked to finish the Beck Depression Inventory test-II (BDI-II) [30] before the start of the experiment. Analysis of BDI showed that the BDI scores in the depressed group were between 14 and 29, corresponding to mild depression, whereas the BDI scores of the normal controls were all lower than 13. Table I shows the demographic characteristics and BDI scores of the two groups. There were no significant differences between two groups in gender ($\chi^2 = 0.403$, $p = 0.525$), age ($t = 0.644$, $p = 0.523$), and education ($t = -1.605$, $p = 0.115$). There was statistical difference in the BDI scale between the two groups, which met the relevant experimental requirements ($p < 0.001$). All participants were rewarded after finishing the experiment.

B. Experimental Paradigm

Fig. 1 showed the sequence of clues and targets used in the visual search paradigm. Fig. 2 showed the demo of the mark display. Table II presented the relationship between the color change of distractors, the number of distractors and the marks in the block. The experiment was divided into four conditions, including G4, G8, R4 and R8, each block has 64 trails. In this experiment, the "+" gaze point will appear first. Later, 4 or 8

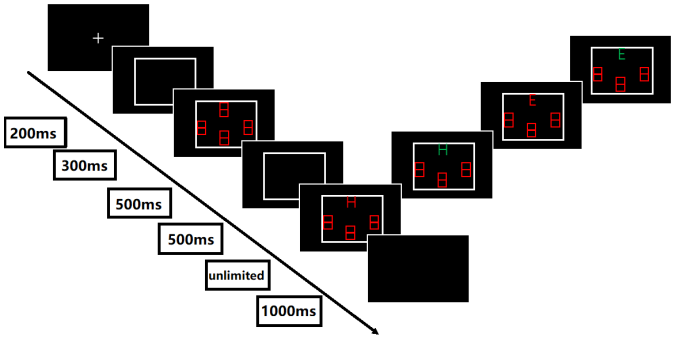

Fig. 1. The sequence of clues and targets in a typical trial from the visual search paradigm.

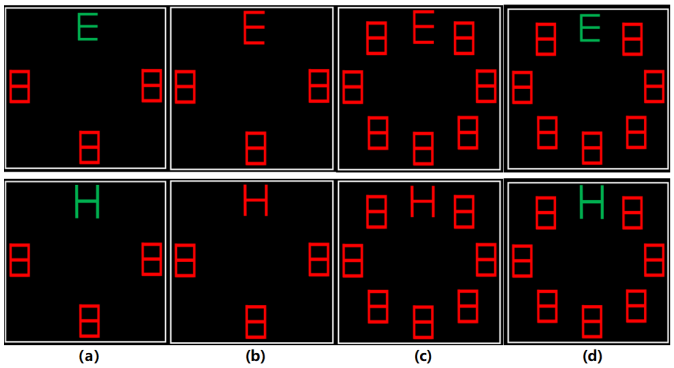

Fig. 2. Demo of the Mark display. Where (a)(b)(c)(d) are G4, R4, G8 and R8 respectively.

"⊟" patterns arranged in a circle will appear on the screen as a position reminder. After 500ms, the "⊟" pattern will change to different letters. Subjects need to find the "E" or "H" among these letters. If the green/red "E" appears, subjects need to press the "Q" key with the index finger of the left hand; if the green/red "H" appears, subjects need to press the "P" key with the index finger of the right hand. After pressing the button, it will automatically enter the next trial. If there is no response for more than 6 seconds, proceed directly to the next trial. Subjects should respond as quickly as possible under each test.

C. EEG Recording and Preprocessing

The EEG data was collected in a quiet, non-electromagnetic interference room. The distance between the subjects and the screen was 60cm. The data was collected by 64-channel electrode cap (Brain Products, Germany). The sampling rate was 1000Hz, the reference electrode was FCz, and the electrode impedance was kept below 10kΩ. Matlab R2020b software, EEGLab14.1.1 toolbox and several plugins were used for data processed. The preprocessing includes the following parts:

(1) Data filtering: the commonly used filter methods to improve the signal qualities includes: Hanning windowed FIR filter [31], Hamming windowed FIR filter [32] and the latest Fourier decomposition method [33], [34]. In this paper, the EEG data was filtered using a Hanning windowed Sinc FIR filter due to its high frequency resolution and less spectrum leakage [35]. The high-pass filter and low-pass filter were set at 0.5 Hz and 40 Hz, respectively, which are the recom-

TABLE II
THE MARK OF DIFFERENT CONDITIONS

Conditions	G4	G8	R4	R8
Mark	11	12	13	14

mended frequencies for the typical experiments to study cognitive, affective, and perceptual processes [36]. And the phase delays introduced by the FIR filters are nullified by applying zero-phase digital filtering based on Matlab function filtfilt(). The filter order was set to the default mode (automatic), which was estimated using heuristic algorithm. After the above processing, low-frequency drift, powerline interference, high-frequency noise and electromyographic artifacts will be effectively removed.

(2) Independent component analysis (ICA) is implemented by using plugins in the EEGLAB tool box under Matlab R2020b software. The Extended Infomax algorithm [37] was adopted to find the demixing matrix and calculate independent components, and its performance was better than Fast ICA [38]. The ICA was run for each subject that included all trials. Then, the Adjust plug-in was used to remove components such as ocular electricity, ECG and EMG due to its automation, absence of constraints on the experimental paradigm, and flexibility to new extensions [39].

(3) In this study, the automatic channels rejection plug-in in EEGLAB was used to remove bad channels. It was found that two subjects each had one bad channel in the MD group (0.083 ± 0.282), while there was no bad channels for every subject in the NC group (0). Then, the location of removed bad channels was interpolated using spherical interpolation. The re-reference is used for the average reference.

(4) There are many ways to extract frequency bands including traditional methods such as Hanning windowed and Hamming windowed, and novel methods such as Fourier decomposition methods [33], [34]. In this paper, Hanning filter was used to extract delta (1-4Hz), theta (4-8Hz), alpha (8-13Hz) and beta (13-30Hz) bands because it has good spectral characteristics and can significantly reduce the errors caused by asynchronous sampling [40].

(5) Extract different types of data segments (G4, G8, R4, and R8) based on the stimuli marks. There are a total of 256 trails, with 64 trails for each condition.

D. Functional Connection Analysis

1) Coupling Method: For the functional connectivity matrix, its nodes are defined by each electrode in the EEG system. Its edges are defined as the connection strength between the different electrodes. Since Imaginary part of coherency (ICoh) method has been proved to be robust under the influence of volume conductivity and has been increasingly used in the research of some mental diseases (such as Alzheimer's disease and autism) [41], [42]. This work utilized this coupling method to construct the functional connection matrix. Details of this method were in the supplementary materials I.

2) Cluster Span Threshold (CST): CST is an unbiased threshold method for network analysis. It achieves the threshold setting by adjusting the ratio of closed triples and open triples to achieve a balance [43], [44] (a brief description of CST was in the supplementary materials I).

3) Graph Theory Analysis: Graph theory analysis has been widely used to explore the abnormalities of various network metrics of depression, because these metrics are reliable and easy to calculate. In this study, the network properties are calculated from the perspective of functional separation and integration. Functional integration features include: Edge Betweenness Centrality (EBC), Node Betweenness Centrality (NBC), and Global Efficiency (GE); functional separation features include: Clustering Coefficient (CC) and Local Efficiency (LE). Mathematical formulas of these metrics are in the supplementary materials I. To explore the differences of network metrics (GE, NBC, LE, EBC, and CC) between the MD and NC groups, the CST method is employed at the individual level. We used the CST to obtain the binary networks from each trial of every subject. Then, network metrics were extracted and averaged from binary networks across all trials for each subject.

4) Hierarchical Clustering Analysis: Clustering is an effective method for studying data node clusters in data mining. In this study, the TAHC method was used to detect clusters in CST. The summary of the TAHC algorithm is as follows: first we use the Dijkstra's shortest path algorithm [45] to compute the geodesic distances matrix of all possible pairs of nodes of given graph, and we use the geodesic distances matrix as an input to the agglomerative hierarchical clustering algorithm. Then the proximity matrix of geodesic matrix is calculated by spearman's rank correlation.

$$\rho = 1 - \frac{6\sum d_i^2}{n(n^2-1)} \tag{1}$$

where ρ is Spearman's rank correlation, and its value is between 0 and 1. n is the sample size, and d_i is the difference between the two rows of each observation.

After that, finding the two closest clusters according to the proximity matrix, and merge them into one cluster. Finally, recalculate similarities between the new cluster and each of the old clusters based on average-linkage clustering and remerge clusters until all nodes are merged into a single cluster. In this study, hierarchical clustering analysis was performed in the group level as the previous research did [20], [23], [24]. We averaged functional connection matrices across trials and subjects to obtain functional connection matrix for each group. Then, CST binarization method was conducted on the functional connection matrix at the group level, which we called group-level CST. In the final, the TAHC method is performed on each group-level CST to obtain the corresponding tree diagram, and the global electrode diagram is used to describe the distribution of nodes and clusters in hierarchical clustering.

There are many evaluation indicators for determining the optimal number of clusters, such as Davies Bouldin Index, Dunn Validity Index, Rand Index, Bootstrap resampling and so on. Since Bootstrap resampling effectively resamples and analyzes the data, the in-depth characteristics of the data itself can be obtained. Therefore in this study, we use Bootstrap resampling technology to determine the optimal number of

clusters [46]. The core of this method is to copy the current data set, the copied data set not only has the attributes of the original data set, but also has the stable characteristics of the original data set. The specific process of Bootstrap resampling technology is as follows: given a data set $Data$ containing n samples, we sample it to generate a data set $Data'$: randomly select a sample from $Data$ each time, copy it into $Data'$, and then the sample is put back into the initial data set $Data$, so that the sample may still be collected in the next sampling; after this process is repeated n times, we get a data set $Data'$ containing n samples. Algorithm 1 is the algorithm for determining the optimal number of clusters using Bootstrap resampling technology. Among them, the selection of the parameters is based on the effective results obtained and proven by previous experiments [46].

E. Statistical Analysis

In this study, three-way repeated measures analysis of variance (ANOVA) was used to test the significant effects on behavioral data and network attributes. Among them, the color change of distractors (C: change is green (G) & no change is red (R)) and the number of distractors (N: 4 & 8) are used as intra-group factors, while group (Group: MD & NC) as inter-subject factors. If interaction between factors is found, a simple-simple effect analysis will be carried out. All analyses are performed at a significance level of 0.05. Independent sample t-test was used to find the difference matrix of two groups. Significance level was set as 0.001, the p values were adjusted for multiple comparisons using the Benjamini Hochberg false discovery rate (FDR) correction. In addition, we would assess the correlation between features (e.g. network metrics, functional connections) with significant differences of two groups and clinical symptoms by Pearson correlation base on permutation test (n = 10000, p = 0.05). Statistical analysis was carried out by SPSS (version 19.0) and Matlab R2020b software.

III. Result

A. Behavioral Data Analysis

In this study, we calculated the reaction time under different conditions for the MD group and the NC group, the reaction time refers to the process from the appearance of the experimental stimulus to the corresponding reaction of the individual. We removed the reaction time of less than 100ms or more than 1000ms trials to minimize the impact of discrete points on the results. Repeated measurement analysis was conducted to compare the reaction time under different stimuli conditions between the two groups. As shown in Table III, a significant group effect was observed on the reaction time ($F(1, 44) = 4.758$, $p = 0.035$), and the reaction time of MD group is significantly higher than NC group for the four conditions. The interaction effect of the color change of distractors (C) × the number of distractors (N) was significant ($F(1, 44) = 80.2$, $p < 0.001$). The effects of C ($F(1, 44) = 377.02$, $p < 0.001$) and N ($F(1, 44) = 8.02$, $p < 0.007$) were significant. In addition, we also compared the accuracy of different stimuli conditions between groups. The interaction effect of N × Group was significant ($F(1, 44) = 4.664$, $p = 0.036$). Moreover, the accuracy of MD group is lower than NC group in each condition.

Algorithm 1 Optimal Cluster Number Determination Algorithm

Input: $Data$ (Raw data)
Output: k^* (Optimal number of clusters)

1: Choose a clustering algorithm;
2: Enter k_1 (minimum number of clusters) and k_2 (maximum number of clusters) for testing;
3: Enter n (n is the number of bootstrap data generated, finally obtaining B_a bootstrap data where $a = 1 \ldots n$);
4: Cluster each bootstrap data;
5: Calculate each $W(P_k, a) = \sum_{k=1}^{K} \sum_{x_i \in c'_k} D^2(x_i, g_k)$, (dispersion within the cluster, K is the number of clusters) c'_k is the k-th cluster, g_k is the cluster center of c'_k, and D is the distance;
6: Calculate ΔW_k (ΔW_k is the observation probability corresponding to the 68% confidence interval on each bootstrap data);
7: Calculate δM_k (it is the clustering tightness on each bootstrap data);
8: Calculate $R_k = a * (\frac{\Delta W_k}{||\Delta W||}) + b * (\frac{\delta M_k}{||\delta M||})$, where $a = 0.75, b = 0.25$; For each cluster k, $||\Delta W|| = \sqrt{\sum_{k=k_1}^{k_2} (\Delta W_k)^2}$, $||\delta M|| = \sqrt{\sum_{k=k_1}^{k_2} (\delta M_k)^2}$;
9: The number of clusters k^* corresponding to the minimum R_k is the real k;

B. Functional Connection Analysis

The distribution of connections with significant differences was shown in Fig. 3 From the results we could find that in the four conditions and four frequency bands, there were more inter-hemispheres connections than intra-hemispheres connections, and the number of long-distance connections were larger than that of the short-distance connections. This showed that when dealing with complex tasks, the MD patients have abnormal information processing pattern. Further to explore the differences of network topology between the MD and NC groups, all the binary brain network matrices obtained from ICoh coupling methods and CST binarization approaches were quantitatively analyzed using graph theory analysis.

C. Network Metrics Analysis

1) Analysis of Group Differences in Network Metrics: This study used network metrics (GE, NBC, LE, EBC, and CC) to analyze the functional brain network topology of MD patients and NC subjects under the visual search task. Results indicated that there was a significant interaction effect of C × Group in the beta band of all five network metrics (CC: [$F(1, 46) = 5.055$, $p = 0.029$], EBC: [$F(1, 46) = 5.207$, $p = 0.027$], GE: [$F(1, 46) = 5.238$, $p = 0.027$], LE: [$F(1, 46) = 4.998$, $p = 0.03$], NBC: [$F(1, 46) = 5.207$, $p = 0.03$]). However, there were no significant interaction effects of the five network metrics in the delta, theta and alpha bands (detailed results

TABLE III
REPEATED MEASUREMENT ANALYSIS OF REACTION TIME AND ACCURACY

	Number of distractors	Color change of distractors				Intersubjective effect	
		No change (Red)		Changed (Green)			
		MD	NC	MD	NC	F	p
Reaction Time	4	706.19±49.06	681.35±214.88	620.67±72.00	610.39±193.79	4.758	**0.035***
	8	751.24±87.19	741.31±121.26	631.70±70.19	615.28±101.93		
Accuracy	4	95.97±4.77%	96.41±3.77%	96.28±4.73%	97.28±3.20%	1.86	0.180
	8	95.06±5.60%	97.47±2.93%	95.51±7.38%	98.25±3.38%		

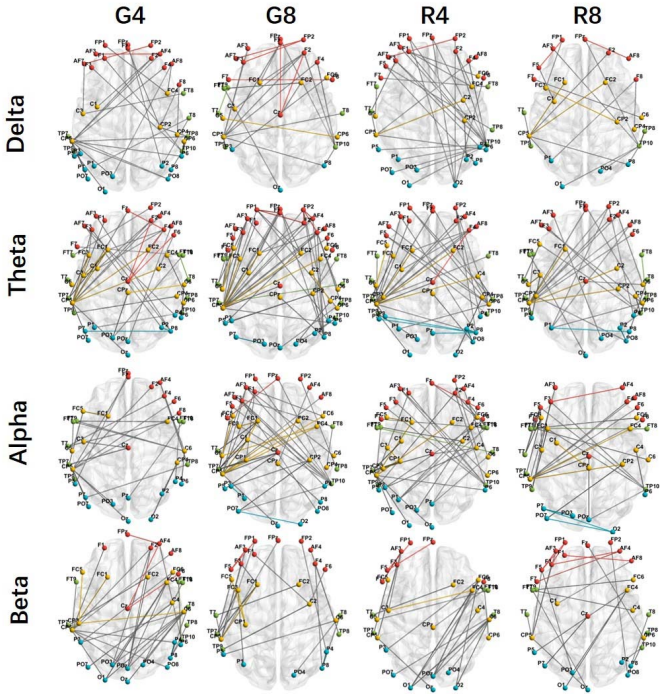

Fig. 3. The distribution of connections with significant differences under the four conditions in four bands based on the ICoh method. Red, yellow, green and blue nodes represent frontal lobe, central lobe, temporal lobe and parietal-occipital lobe, respectively. The colored line indicates that there are significant differences in the connected edges of this area, and the black line indicates that there are significant differences in the connected edges of different regions. Statistic value $p<0.001$.

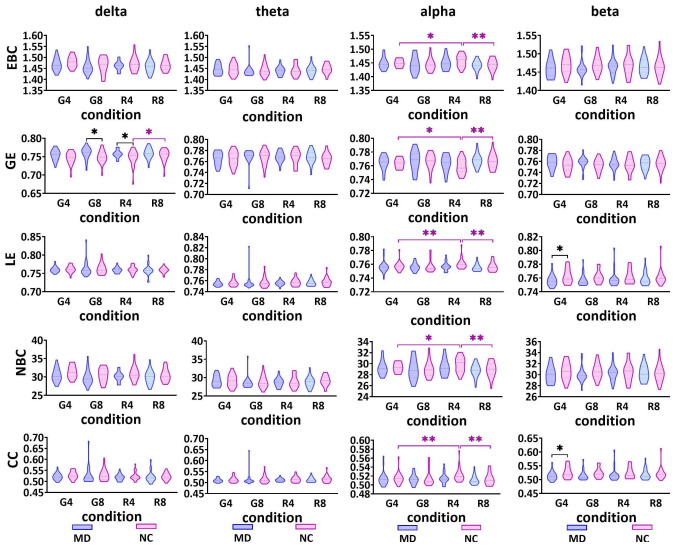

Fig. 4. Statistical results of five network metrics in four bands based on the ICoh+CST method. Blue and pink * represent intra-group difference in MD group and NC group, respectively. Black * indicates there is a significant difference between MD and NC groups. Statistic value $p<0.05$.

TABLE IV
SIMPLE-SIMPLE EFFECT ANALYSIS OF THE FIVE NETWORK METRICS IN THE BETA BAND

Color	EBC		GE		LE		NBC		CC	
	F	p	F	p	F	p	F	p	F	p
G	2.803	0.101	2.820	0.100	**5.457**	**0.024**	2.803	0.101	**5.354**	**0.025**
R	0.076	0.784	0.076	0.784	0.802	0.375	0.076	0.784	0.744	0.393

were in the supplementary materials III). So in the following work, the simple-simple effect analysis was only performed in the beta frequency band. As shown in Fig. 4, in the beta band under the G4 condition, the LE and CC metrics of MD group was significant lower than that of NC group (LE: MD $= 0.756 \pm 0.008$, NC $= 0.763 \pm 0.011$, $p = 0.016$; CC: MD $= 0.513 \pm 0.016$, NC $= 0.527 \pm 0.021$, $p = 0.016$).

In order to investigate the nature of the interaction between the two factors, a simple-simple effect analysis was performed. As shown in Table IV, a significant interaction of the changed color of distractors (G) × Group was observed on the LE and CC (LE: $F(1, 46) = 5.457$, $p = 0.024$; CC: $F(1, 46) = 5.354$, $p = 0.025$). And it can be inferred from Fig. 2 that patients with MD were less sensitive to the change of distractors' color than the NC.

Though there were multi-factor interaction differences of EBC, GE, and NBC in the beta band, there was no significant difference between the two groups after a simple-simple effect analysis. To explain this phenomenon, we did a simple interaction effect analysis. The results are shown in Table V. It was found that there was intra-group marginal significance of EBC, GE and NBC in MD group regardless of the change of the color of distractors. Therefore, it can be considered that the two-factor interaction differences shown by these three network metrics in the beta band are due to individual differences within the group.

In the meantime, we also calculated the sparsity of the networks obtained from CST binarization method. Results indicated that there was no significant difference between MD group and NC group (detailed results were provided in the supplementary materials II), which proved that CST was an effective method to explore the aberrant brain network topology structure of MD.

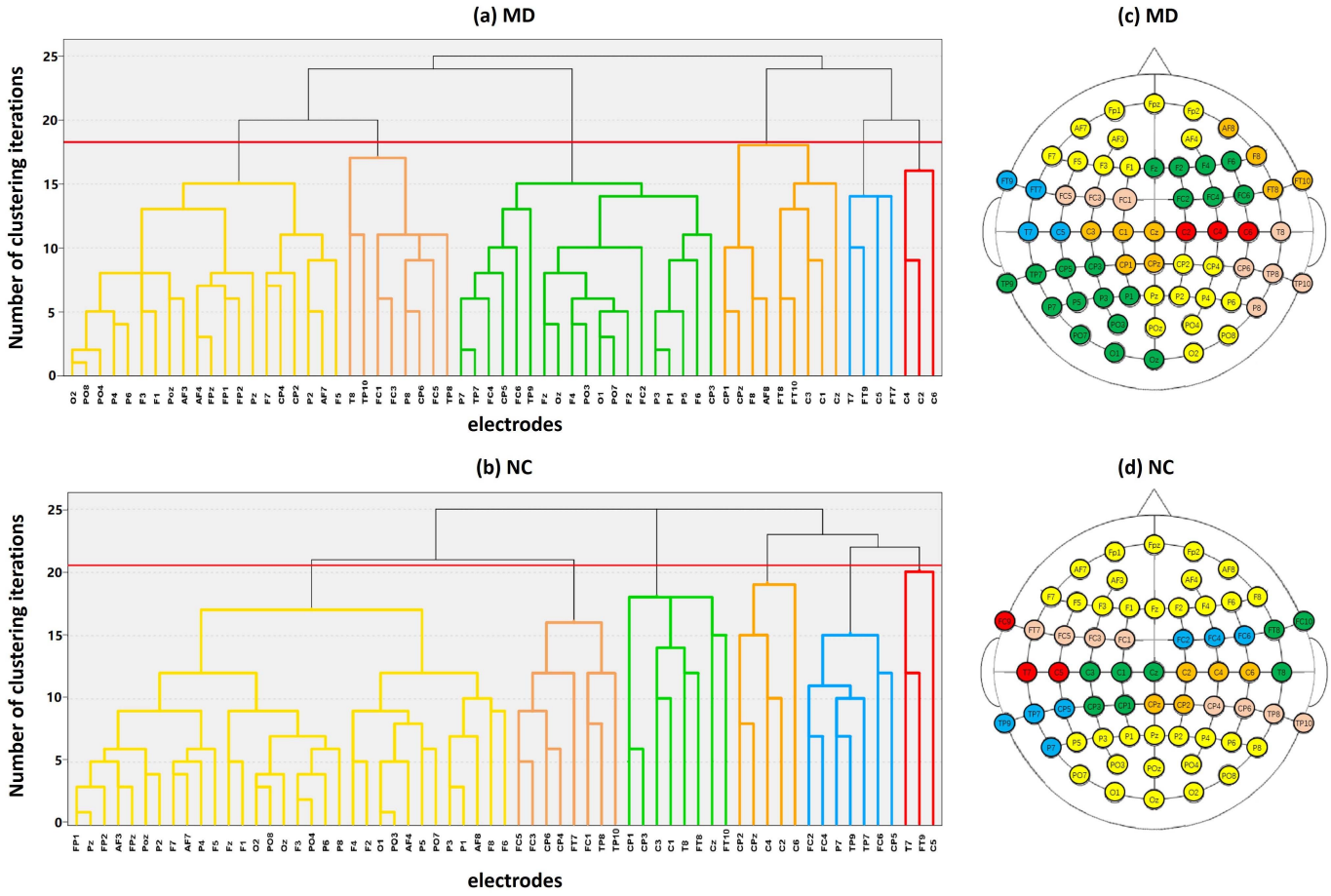

Fig. 5. The hierarchical clustering graphs and brain distribution map of clusters of MD and NC groups based on TAHC algorithm in the beta band under the G4 condition.

TABLE V
SIMPLE INTERACTION ANALYSIS OF THE THREE NETWORK METRICS OF EBC, GE AND NBC IN THE BETA BAND

	EBC		GE		NBC	
	MD	NC	MD	NC	MD	NC
Color (p-value)	0.071	0.174	0.069	0.177	0.071	0.174

2) Analysis of Intra-Group Differences in Network Metrics: From Fig. 4, it was found that in alpha band, there were significant intra-group differences of the five network metrics (GE, LE, EBC, NBC and CC) of NC group between R4 and R8 conditions and between G4 and R4 conditions. And in delta band, there was significant intra-group difference of the network metric GE of NC group between R4 and R8 conditions.

In addition, we also analyzed the network metrics calculated from ICoh coupling method and MST binarization method. However, no significant group and intra-group differences of network metrics were found based on this method (detailed results were in the supplementary materials III), which demonstrated the superiority of ICoh + CST. And based on this method, we found that there were significant differences of CC and LE between the two groups in the beta band under the G4 condition. Therefore, the hierarchical structure of the two groups will be further explored on this condition.

D. Hierarchical Clustering Analysis

TAHC algorithm was applied to construct the hierarchical clustering of the functional connection network for both groups in the beta band under the G4 condition. And the optimal number of clusters 6 was obtained based on the optimal cluster number determination algorithm (see Fig. 5(a) and (b)). To display the details of the cluster result, we plotted brain distribution map of clusters in Fig. 5(c) and (d). It was found that the MD group tended to cluster according to the physical structure of the brain, corresponding to the left and right hemisphere, whereas the NC group tended to cluster according to the functional structure of the brain, corresponding to different functional regions. More importantly, we found that a large number of electrodes in frontal and parieto-occipital regions were clustered into a community in the NC group. However, for the MD group, both the left and right frontal were clustered with the opposite parietal-occipital regions into a community, respectively. And from brain distribution map of the clusters, we speculated that patients with MD might have brain asymmetry.

E. Brain Asymmetry Analysis

To explore the brain asymmetry of MD patients in the beta band under the G4 condition, this study divided the brain into different regions including Left-frontal (LF), Right-

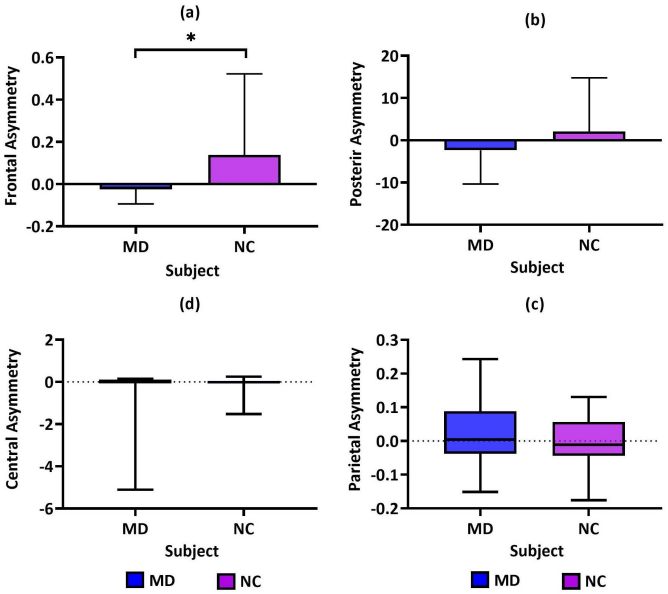

Fig. 6. Brain asymmetry of MD and NC groups in the beta band under the G4 condition.

frontal (RF), Left-central (LC), Right-central (RC), Left-temporal (LT), Right-temporal (RT), Left-parietal-occipital (LPO), Right-parietal-occipital (RPO) according to their anatomical positions [47] (see Table S1 in the supplementary materials III). Specific hypotheses were tested using one-way ANOVA. The significant level p was 0.05. Brain asymmetry indices were calculated by subtracting the natural log of the power of the left hemisphere electrodes from that of the homologous right hemisphere electrodes [48]:

$$\frac{\ln(right(power)) - \ln(left(power))}{\ln(right(power)) + \ln(left(power))} \quad (2)$$

In this way, positive scores indicated right hemispheric electrodes had greater beta power than the left hemispheric electrodes. Due to the inverse relationship between beta power and cortical activity, the positive scores represented relative greater activity in the left-sided brain region, while the negative scores represented relative greater activity in the right-sided brain region [49]. The brain asymmetry results of the MD group and the NC group were shown in Fig. 6. It was found that the left frontal activity in MD group (Mean $= -0.256$, Std $= 0.698$) was significantly lower ($F(1, 46) = 4.167$, $p = 0.047$) than that in NC group (Mean $= 0.139$, Std $= 0.384$). However, there was no difference in other brain regions between the two groups.

F. Correlation Analysis

According to the obtained statistic results, correlation analysis was conducted between features that having significant differences (CC, LE, frontal asymmetry (F_A), and the average functional connection value between the left frontal lobe and right parietal occipital (LF_RPO) and between the right frontal lobe and left parietal occipital (RF_LPO)) and BDI scores. Results were shown in Fig. 7, in the beta band, LF_RPO ($r = 0.314$, $p = 0.030$) was significantly positive correlated with the BDI scores.

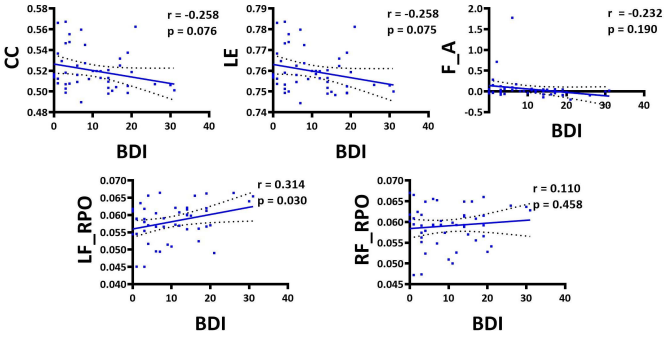

Fig. 7. The results of the correlation between the features with signi-ficant differences and the BDI scores in the beta band under G4 condition. r represents the correlation coefficient, p is the statistical value.

IV. Discussion

This study adopted novel functional brain network analysis method and hierarchical clustering algorithm for the first time to systematically explore the abnormal brain topology of patients with MD under the visual search paradigm. Our main findings were: (1) Behavioral data analysis showed that compared to the NC group, the MD group exhibited longer reaction time; (2) Functional connection analysis indicated that inter-hemispheric long-distance connections accounted for a larger proportion in significant differences connections between the two groups; (3) Network attribute analysis showed that the LE and CC of the MD group were significantly lower than that of the NC group under the G4 condition in beta band; (4) Hierarchical clustering analysis indicated that MD group lost clustering structure of the frontal region and parietal-occipital region, and the average value of long-distance connections between left frontal and right parietal-occipital lobes was significantly positive correlated with the BDI scores; (5) Analysis of brain asymmetry showed that the MD group existed frontal asymmetry.

A. Abnormal Behavioral Indicators in MD

Our results showed that compared to NC group, MD group had significant longer reaction time during the visual search task, which are consistent with previous studies. For example, Hammar ÅSA [50]found that when the target stimulus is significantly different from the surrounding analytical stimulus, as the number of surrounding distractors increases, it takes longer for depressive group to recognize targets, and their accuracy is slightly lower than that of the control group. Other studies had pointed out that the continuous deployment selectivity of spatial attention in depressive patients was impaired. When depressive patients performed the visual search task, regardless of whether the stimulus was novel or non-novel target, depressive patients showed severe lack of comparative search ability. Therefore, when a novel target appeared, patients with depression had delayed and biased judgments on the novelty of the target, and exhibited attention-biased behavior [51]. Julia F also found that when the target was defined by a combination of characteristics (e.g. color and shape), the depressive group showed a severe lack of comparative search ability [52]. Previous research has verified

the validity of our results. Thus we believed that the MD group had selective impairment in the continuous deployment of spatial attention, which resulted in the MD group probably in need of more information processing efforts in the face of intervention task.

B. Abnormal Functional Brain Network Structure in MD

There is increasing evidence that functional interactions between different brain regions are mediated by their synchronization oscillations. These interactions are believed to be associated with various cognitive functions as well as the integration of information in the healthy brain [53], [54]. For example, Donner TH. *et al.* found that long-range interareal linkage of distributed areas in NeuroCognitive Networks was mediated by synchronous oscillations of beta band [55]. And inter-hemispheric communication is an important part of cognitive and emotional processing [56], [57]. Especially, when performing complex tasks, the inter-hemispheric communication is necessary [58]. In this study, when performing the visual search task, we found that in the functional connections with significant differences between the MD and NC groups, the inter-hemispheric long-distance connections occupied a larger proportion compared to the intra-hemispheric short-distance connections. Similar finding showed the long-distance connections between the pre-frontal area and the parietal area to the temporal area showed inter-group differences in the theta band [59]. So the results indicated that when performing complex tasks, patients with MD had abnormal inter-hemispheres interaction.

The CC and LE are measures of the local information processing of the network. Our findings indicated that compared with NC group, MD group exhibited decreased LE and CC network metrics of beta band in the G4 condition, which suggested that efficiency of information segregation in MD group was decreased during the processing of the complex task. Li *et al.* found that compared to the NC group, MD group had a lower CC network metric in beta band for exploring the complexity network under emotion processing task [60]. Some studies also found that patients with depression had decreased nodal efficiency and CC [51], [61], [62]. Other studies found that there were decreased CC and LE and increased characteristic path length and GE of patients with depression [63], [64], which supported the speculation that the brain network of patients with depression tended to be random [65]. However, this study didn't observe significant differences of GE between the two groups [51], [66], [67]. In addition, our findings are contrary to other studies, which showed that patients with depression had increased CC and LE compared with NC group [67]. These discrepancies between different studies might be caused by the individual differences and methodological differences. Thus, more research is needed to reproduce these findings.

Further to explore the hierarchical structure of the MD and NC groups in the beta band under the G4 condition, it was found that there were different clusters between the two groups. For the MD group, the hierarchical structure of the frontal lobe and parieto-occipital lobe was destroyed, where the left frontal lobe and the right parieto-occipital lobe, the right frontal lobe and the left parieto-occipital lobe were clustered into a community, respectively. For the NC group, the frontal and parieto-occipital lobe were clustered into a community. Relevant study revealed that the nodes in frontal regions of the depression group were divided into two clusters in the left forehead and the right forehead, while the NC group were clustered into a community [24]. Normal brain organization is considered to be determined by the economic trade-off between minimizing costs (high-cost hubs and long-distance connections) and information processing efficiency [68]. Buzsáki *et al.* found that, in a normal brain, direct connections between brain regions that are far away in space support faster and more direct information transmission [69]. However, our research found that the MD group achieved long-distance connections between brain regions at the cost of interrupting the intra-cluster connections between the frontal lobe cluster and the parieto-occipital cluster, which might lead to high-cost hubs and long-distance connections in the brain tissue, thus breaking the aforementioned balance between cost minimization and information processing efficiency. More importantly, the average functional connection value between the left frontal lobe and right parietal occipital was significantly correlated with the BDI scores, indicating the more severe the depression, the higher the average functional connection value, which suggested that the average functional connection value of this cluster might be an underlying biomarker for probable MD identification. And the results are supported by relevant studies [70], [71]. In addition, from the cluster results, the destruction of the frontal lobe cluster and the parieto-occipital lobe cluster (that is, the lack of connection between the hemispheres) might explain why there were significant differences in the LE and CC network metrics between MD and NC groups.

C. Abnormal Brain Symmetry in MD

Frontal lobe and central lobe play an important role in attention processing [72]. Many EEG studies have found frontal asymmetry existed in the patients with depression. For example, Bruder and Kemp found that the depressive patients generally had lower alpha power in the right frontal lobe than in the left frontal lobe [73], [74]. Spironelli *et al.* found depression patients showed a lack of frontal asymmetry and a significantly lower activation of left frontal lobe in the beta band under state-resting [75]. VadimZotev *et al.* found the depressive patients had frontal EEG asymmetry in the high-beta band under emotion self-regulation task [76]. Similar results were found in our study, MD patients had frontal asymmetry, where the power of right frontal lobe was lower than that of left frontal lobe, meaning that the relative activity of the right frontal lobe was higher than that of left frontal lobe. There is considerable evidence that affective behavior is related to frontal activation asymmetries, with negative affect or withdrawal behaviors being associated with right frontal activation, and positive affect or approach behaviors being associated with left frontal activation [77]. So we considered that compared to the NC group, patients with MD had the negative affect bias.

V. Limitations and Future Directions

Several issues need to be further addressed. First, the sample size was relatively small that this study can't stratify the patients by depressive subtypes. Larger sample is required to verify our results and to explore neurophysiological aspects of different depressive levels. Second, this research for the functional brain networks was in sensor level. In order to make the analysis of functional brain network can be more refined and accurate, we will explore the distribution in the source space of EEG signal based on source location technology in the future work. Finally, a possible disadvantage of the Hanning filter is that it does not provide a sharp cutoff to decompose the EEG data into rhythms. Relevant studies demonstrated that the Fourier decomposition approach [33], [34] could solve this problem. Therefore, in the further, we will try to use this method to decompose the EEG data into rhythms.

VI. Conclusion

This study adopted novel functional brain network analysis method and hierarchical clustering algorithm for the first time to systematically explore the differences of brain topological structure between patients with MD and normal controls while they were performing the visual search paradigm. We found that in the functional connections with significant differences between the two groups, the inter-hemispheric long-distance connections occupied a larger proportion compared to the intra-hemispheric short-distance connections, these indicated when performing complex tasks, the patients with MD had abnormal inter-hemispheric communication. Especially in the beta band, compared to NC group, hierarchical structure of the frontal lobe and parieto-occipital lobe was destroyed in the MD group, where the left frontal lobe and the right parieto-occipital lobe, the right frontal lobe and the left parieto-occipital lobe were clustered into a community, respectively. And the average functional connection value between the left frontal lobe and right parietal occipital was significantly correlated with the BDI scores, which indicated that the average connection value of this cluster might be a potential electrophysiological characteristic for probable MD identification. Meanwhile, patients with MD showed significantly lower local efficiency and clustering coefficient, and frontal asymmetry. These results further confirmed that there exist abnormal cognitive processing mechanism of MD patients. In summary, these findings provided insights into our under-standing of aberrant topology organization in functional brain networks of patients with MD.

References

[1] G. Ouyang *et al.*, "The global, regional, and national burden of pancreatitis in 195 countries and territories, 1990–2017: A systematic analysis for the global burden of disease study 2017," *BMC Med.*, vol. 5, no. 1, pp. 17–30, Dec. 2020.

[2] M. Kennis, L. Gerritsen, M. van Dalen, A. Williams, P. Cuijpers, and C. Bockting, "Prospective biomarkers of major depressive disorder: A systematic review and meta-analysis," *Mol. Psychiatry*, vol. 25, no. 2, pp. 321–338, Feb. 2020.

[3] D. S. Hasin *et al.*, "Epidemiology of adult DSM-5 major depressive disorder and its specifiers in the United States," *JAMA Psychiatry*, vol. 75, no. 4, pp. 336–346, 2018.

[4] R. Kerestes, C. G. Davey, K. Stephanou, S. Whittle, and B. J. Harrison, "Functional brain imaging studies of youth depression: A systematic review," *NeuroImage, Clin.*, vol. 4, pp. 209–231, Jan. 2014.

[5] L. T. Park and C. A. Zarate, Jr., "Depression in the primary care setting," *New England J. Med.*, vol. 380, no. 6, pp. 559–568, 2019.

[6] M. Chmielewski, L. A. Clark, R. M. Bagby, and D. Watson, "Method matters: Understanding diagnostic reliability in DSM-IV and DSM-5," *J. Abnormal Psychol.*, vol. 124, no. 3, p. 764, 2015.

[7] P. Wu *et al.*, "Mapping ICD-10 and ICD-10-CM codes to phecodes: Workflow development and initial evaluation," *JMIR Med. Informat.*, vol. 7, no. 4, Nov. 2019, Art. no. e14325.

[8] X. Li *et al.*, "EEG-based mild depression recognition using convolutional neural network," *Med. Biol. Eng. Comput.*, vol. 57, no. 6, pp. 1341–1352, Feb. 2019.

[9] D. E. Van *et al.*, "Opportunities and methodological challenges in EEG and MEG resting state functional brain network research," *Clin. Neurophysiol.*, vol. 126, no. 8, pp. 1468–1481, 2015.

[10] J. Brakowski *et al.*, "Resting state brain network function in major depression—Depression symptomatology, antidepressant treatment effects, future research," *J. Psychiatric Res.*, vol. 92, pp. 147–159, Sep. 2017.

[11] C.-G. Yan *et al.*, "Reduced default mode network functional connectivity in patients with recurrent major depressive disorder," *Proc. Nat. Acad. Sci. USA*, vol. 116, no. 18, pp. 9078–9083, 2019.

[12] B. He *et al.*, "Electrophysiological brain connectivity: Theory and implementation," *IEEE Trans. Biomed. Eng.*, vol. 66, no. 7, pp. 2115–2137, Jul. 2019.

[13] A. T. Drysdale *et al.*, "Resting-state connectivity biomarkers define neurophysiological subtypes of depression," *Nature Med.*, vol. 23, no. 1, pp. 28–38, Jan. 2017.

[14] A. A. Fingelkurts and A. A. Fingelkurts, "Altered structure of dynamic electroencephalogram oscillatory pattern in major depression," *Biol. Psychiatry*, vol. 77, no. 12, pp. 1050–1060, Jun. 2015.

[15] S. Sun *et al.*, "Graph theory analysis of functional connectivity in major depression disorder with high-density resting state EEG data," *IEEE Trans. Neural Syst. Rehabil. Eng.*, vol. 27, no. 3, pp. 429–439, Mar. 2019.

[16] J. Zhang *et al.*, "Pattern classification of large-scale functional brain networks: Identification of informative neuroimaging markers for epilepsy," *PLoS ONE*, vol. 7, no. 5, May 2012, Art. no. e36733.

[17] J. DelEtoile and H. Adeli, "Graph theory and brain connectivity in Alzheimer's disease," *Neuroscientist*, vol. 23, no. 6, pp. 616–626, 2017.

[18] K. Smith, H. Azami, M. A. Parra, J. M. Starr, and J. Escudero, "Cluster-span threshold: An unbiased threshold for binarising weighted complete networks in functional connectivity analysis," in *Proc. 37th Annu. Int. Conf. IEEE Eng. Med. Biol. Soc. (EMBC)*, Aug. 2015, pp. 2840–2843.

[19] K. Smith, D. Abasolo, and J. Escudero, "A comparison of the cluster-span threshold and the union of shortest paths as objective thresholds of EEG functional connectivity networks from beta activity in Alzheimer's disease," in *Proc. 38th Annu. Int. Conf. IEEE Eng. Med. Biol. Soc. (EMBC)*, Aug. 2016, pp. 2826–2829.

[20] M. Yu *et al.*, "Hierarchical clustering in minimum spanning trees," *Chaos, Interdiscipl. J. Nonlinear Sci.*, vol. 25, no. 2, 2015, Art. no. 023107.

[21] R. F. Betzel and D. S. Bassett, "Multi-scale brain networks," *NeuroImage*, vol. 160, pp. 73–83, Oct. 2017.

[22] O. Sporns and R. F. Betzel, "Modular brain networks," *Annu. Rev. Psychol.*, vol. 67, pp. 613–640, Jan. 2016.

[23] D. J. Smit, C. J. Stam, D. Posthuma, D. I. Boomsma, and E. J. De Geus, "Heritability of 'small-world' networks in the brain: A graph theoretical analysis of resting-state eeg functional connectivity," *Hum. Brain Mapping*, vol. 29, no. 12, pp. 1368–1378, 2008.

[24] X. Li *et al.*, "A resting-state brain functional network study in MDD based on minimum spanning tree analysis and the hierarchical clustering," *Complexity*, vol. 2017, pp. 1–11, Jul. 2017.

[25] K. Tummeltshammer and D. Amso, "Top-down contextual knowledge guides visual attention in infancy," *Develop. Sci.*, vol. 21, no. 4, Jul. 2018, Art. no. e12599.

[26] S. Hahn, C. Carlson, S. Singer, and S. D. Gronlund, "Aging and visual search: Automatic and controlled attentional bias to threat faces," *Acta Psychologica*, vol. 123, no. 3, pp. 312–336, Nov. 2006.

[27] A. Byrne and M. W. Eysenck, "Trait anxiety, anxious mood, and threat detection," *Cognition Emotion*, vol. 9, no. 6, pp. 549–562, Nov. 1995.

[28] C. Wang, L. Hu, T. Talhelm, and X. Zhang, "The effects of colour complexity and similarity on multiple object tracking performance," *Quart. J. Exp. Psychol.*, vol. 72, no. 8, pp. 1903–1912, Aug. 2019.

[29] E. De Voogd *et al.*, "Online attentional bias modification training targeting anxiety and depression in unselected adolescents: Short-and long-term effects of a randomized controlled trial," *Behav. Res. Therapy*, vol. 87, pp. 11–22, Dec. 2016.

[30] Z. E. García-Batista, K. Guerra-Peña, A. Cano-Vindel, S. X. Herrera-Martínez, and L. A. Medrano, "Validity and reliability of the beck depression inventory (BDI-II) in general and hospital population of Dominican republic," *PLoS ONE*, vol. 13, no. 6, Jun. 2018, Art. no. e0199750.

[31] A. Widmann, E. Schröger, and B. Maess, "Digital filter design for electrophysiological data—A practical approach," *J. Neurosci. Methods*, vol. 250, pp. 34–46, Jul. 2015.

[32] J. Kaiser and R. Hamming, "Sharpening the response of a symmetric nonrecursive filter by multiple use of the same filter," *IEEE Trans. Acoust., Speech, Signal Process.*, vol. ASSP-25, no. 5, pp. 415–422, Oct. 1977.

[33] P. Singh, S. D. Joshi, R. K. Patney, and K. Saha, "The Fourier decomposition method for nonlinear and non-stationary time series analysis," *Proc. Roy. Soc. A, Math., Phys. Eng. Sci.*, vol. 473, no. 2199, Mar. 2017, Art. no. 20160871.

[34] A. Singhal, P. Singh, B. Fatimah, and R. B. Pachori, "An efficient removal of power-line interference and baseline wander from ECG signals by employing Fourier decomposition technique," *Biomed. Signal Process. Control*, vol. 57, Mar. 2020, Art. no. 101741.

[35] K. F. Chen and Y. F. Li, "Combining the Hanning windowed interpolated FFT in both directions," *Comput. Phys. Commun.*, vol. 178, no. 12, pp. 924–928, Jun. 2008.

[36] S. J. Luck, *An Introduction to Event-Related Potential Technique*. Cambridge, MA, USA: MIT Press, 2014.

[37] T.-W. Lee, "Independent component analysis," in *Independent Component Analysis*. Boston, MA, USA: Springer, 1998, pp. 27–66.

[38] F. Djouad *et al.*, "Microenvironmental changes during differentiation of mesenchymal stem cells towards chondrocytes," *Arthritis Res. Therapy*, vol. 9, no. 2, pp. 1–12, 2007.

[39] A. Mognon, J. Jovicich, L. Bruzzone, and M. Buiatti, "ADJUST: An automatic EEG artifact detector based on the joint use of spatial and temporal features," *Psychophysiology*, vol. 48, no. 2, pp. 229–240, Feb. 2011.

[40] G. Zhu, K. Zhou, L. Lu, Y. Li, H. Xi, and Q. Zeng, "Online monitoring of power cables tangent delta based on low-frequency signal injection method," *IEEE Trans. Instrum. Meas.*, vol. 70, pp. 1–8, 2021.

[41] L. G. Domínguez, J. Stieben, J. L. Pérez Velázquez, and S. Shanker, "The imaginary part of coherency in autism: Differences in cortical functional connectivity in preschool children," *PLoS ONE*, vol. 8, no. 10, Oct. 2013, Art. no. e75941.

[42] C. J. Stam, G. Nolte, and A. Daffertshofer, "Phase lag index: Assessment of functional connectivity from multi channel EEG and MEG with diminished bias from common sources," *Hum. Brain Mapping.*, vol. 28, no. 11, pp. 1178–1193, Nov. 2007.

[43] O. Sporns, "Network attributes for segregation and integration in the human brain," *Current Opinion Neurobiol.*, vol. 23, no. 2, pp. 162–171, Apr. 2013.

[44] M. P. van den Heuvel and O. Sporns, "Network hubs in the human brain," *Trends Cogn. Sci.*, vol. 17, pp. 683–696, Dec. 2013.

[45] S. Broumi, A. Bakal, M. Talea, F. Smarandache, and L. Vladareanu, "Applying Dijkstra algorithm for solving neutrosophic shortest path problem," in *Proc. Int. Conf. Adv. Mech. Syst. (ICAMechS)*, Nov. 2016, pp. 412–416.

[46] A. K. Jain and J. V. Moreau, "Bootstrap technique in cluster analysis," *Pattern Recognit.*, vol. 20, no. 5, pp. 547–568, Jan. 1987.

[47] Q. Zhao *et al.*, "Nonlinear dynamic analysis of resting EEG alpha activity for heroin addicts," in *Proc. IEEE Int. Conf. Bioinf. Biomed. (BIBM)*, Dec. 2016, pp. 533–537.

[48] D. Mathersul, L. M. Williams, P. J. Hopkinson, and A. H. Kemp, "Investigating models of affect: Relationships among EEG alpha asymmetry, depression, and anxiety," *Emotion*, vol. 8, no. 4, p. 560, 2008.

[49] J. A. Coan and J. J. B. Allen, "Frontal EEG asymmetry as a moderator and mediator of emotion," *Biol. Psychol.*, vol. 67, nos. 1–2, pp. 7–50, 2004.

[50] A. Hammar, "Automatic and effortful information processing in unipolar major depression," *Scandin. J. Psychol.*, vol. 44, no. 5, pp. 409–413, Dec. 2003.

[51] Y. Li, D. Cao, L. Wei, Y. Tang, and J. Wang, "Abnormal functional connectivity of EEG gamma band in patients with depression during emotional face processing," *Clin. Neurophysiol.*, vol. 126, no. 11, pp. 2078–2089, Nov. 2015.

[52] J. Fellrath, V. Blanche-Durbec, A. Schnider, A.-S. Jacquemoud, and R. Ptak, "Visual search in spatial neglect studied with a preview paradigm," *Frontiers Hum. Neurosci.*, vol. 6, p. 93, Apr. 2012.

[53] Y. Urakami, "Relationships between sleep spindles and activities of cerebral cortex as determined by simultaneous EEG and MEG recording," *J. Clin. Neurophysiol.*, vol. 25, no. 1, pp. 13–24, 2008.

[54] C. J. Stam and J. C. Reijneveld, "Graph theoretical analysis of complex networks in the brain," *Nonlinear Biomed. Phys.*, vol. 1, no. 1, pp. 1–19, Dec. 2007.

[55] T. H. Donner and M. Siegel, "A framework for local cortical oscillation patterns," *Trends Cogn. Sci.*, vol. 15, no. 5, pp. 191–199, May 2011.

[56] R. J. Compton, K. Feigenson, and P. Widick, "Take it to the bridge: An interhemispheric processing advantage for emotional faces," *Cognit. Brain Res.*, vol. 24, no. 1, pp. 66–72, Jun. 2005.

[57] R. Toro, P. T. Fox, and T. Paus, "Functional coactivation map of the human brain," *Cerebral Cortex*, vol. 18, no. 11, pp. 2553–2559, Nov. 2008.

[58] D. H. Weissman and M. T. Banich, "The cerebral hemispheres cooperate to perform complex but not simple tasks," *Neuropsychology*, vol. 14, no. 1, pp. 41–59, 2000.

[59] M. A. Quraan *et al.*, "EEG power asymmetry and functional connectivity as a marker of treatment effectiveness in DBS surgery for depression," *Neuropsychopharmacology*, vol. 39, no. 5, pp. 1270–1281, Apr. 2014.

[60] X. Li, R. La, Y. Wang, B. Hu, and X. Zhang, "A deep learning approach for mild depression recognition based on functional connectivity using electroencephalography," *Frontiers Neurosci.*, vol. 14, p. 192, Apr. 2020.

[61] Y. Li *et al.*, "Beta oscillations in major depression—Signalling a new cortical circuit for central executive function," *Sci. Rep.*, vol. 7, no. 1, pp. 1–15, Dec. 2017.

[62] H. Li, H. Zhou, Y. Yang, H. Wang, and N. Zhong, "More randomized and resilient in the topological properties of functional brain networks in patients with major depressive disorder," *J. Clin. Neurosci.*, vol. 44, pp. 274–278, Oct. 2017.

[63] D. J. Watts and S. H. Strogatz, "Collective dynamics of 'small-world' networks," *Nature*, vol. 393, nos. 66–84, pp. 440–442, 1998.

[64] O. Sporns, "The human connectome: A complex network," *Ann. New York Acad. Sci.*, vol. 1224, no. 1, pp. 109–125, Apr. 2011.

[65] J. Chen, H. Guo, C. Cheng, X. Cao, J. Xiang, and K. Zhang, "Resting-state functional connectivity abnormalities in first-onset unmedicated depression," *Neural Regener. Res.*, vol. 9, no. 2, p. 153, 2014.

[66] Q. Gong and Y. He, "Depression, neuroimaging and connectomics: A selective overview," *Biol. Psychiatry*, vol. 77, no. 3, pp. 223–235, 2015.

[67] N. Fogelson, P. Diaz-Brage, L. Li, A. Peled, and E. Klein, "Functional connectivity abnormalities during processing of predictive stimuli in patients with major depressive disorder," *Brain Res.*, vol. 1727, Jan. 2020, Art. no. 146543.

[68] E. Bullmore and O. Sporns, "The economy of brain network organization," *Nature Rev., Neurosci.*, vol. 13, pp. 336–349, May 2012.

[69] G. Buzsáki, C. Geisler, D. A. Henze, and X.-J. Wang, "Interneuron diversity series: Circuit complexity and axon wiring economy of cortical interneurons," *Trends Neurosci.*, vol. 27, no. 4, pp. 186–193, Apr. 2004.

[70] A. Crowther *et al.*, "Resting-state connectivity predictors of response to psychotherapy in major depressive disorder," *Neuropsychopharmacology*, vol. 40, no. 7, pp. 1659–1673, Jun. 2015.

[71] A. F. Leuchter, I. A. Cook, A. M. Hunter, C. Cai, and S. Horvath, "Resting-state quantitative electroencephalography reveals increased neurophysiologic connectivity in depression," *PLoS ONE*, vol. 7, no. 2, Feb. 2012, Art. no. e32508.

[72] H. Iddas and K. Iramina, "Directed EEG functional connectivity features to reveal different attention indexes using hierarchical clustering," *IEEE Access*, vol. 9, pp. 59328–59335, 2021.

[73] G. E. Bruder *et al.*, "Regional brain asymmetries in major depression with or without an anxiety disorder: A quantitative electroencephalographic study," *Biol. Psychiatry*, vol. 41, no. 9, pp. 939–948, May 1997.

[74] A. Kemp *et al.*, "Disorder specificity despite comorbidity: Resting EEG alpha asymmetry in major depressive disorder and post-traumatic stress disorder," *Biol. Psychol.*, vol. 85, pp. 350–354, Oct. 2010.

[75] C. Spironelli *et al.*, "Evidence of language-related left hypofrontality in major depression: An EEG beta band study," *Sci. Rep.*, vol. 10, no. 1, pp. 1–12, Dec. 2020.

[76] V. Zotev, A. Mayeli, M. Misaki, and J. Bodurka, "Emotion self-regulation training in major depressive disorder using simultaneous real-time fMRI and EEG neurofeedback," *NeuroImage, Clin.*, vol. 27, Jan. 2020, Art. no. 102331.

[77] R. E. Wheeler, R. J. Davidson, and A. J. Tomarken, "Frontal brain asymmetry and emotional reactivity: A biological substrate of affective style," *Psychophysiology*, vol. 30, no. 1, pp. 82–89, 1993.